

1 **Effects of changes in moisture source and the upstream rainout on stable**  
2 **isotopes in precipitation — a case study in Nanjing, East China**

3  
4 Yanying Tang<sup>1</sup>, Hongxi Pang<sup>1\*</sup>, Wangbin Zhang<sup>1</sup>, Yaju Li<sup>1</sup>, Shuangye Wu<sup>1,2</sup>, Shugui Hou<sup>1\*</sup>

5 1.Key Laboratory of Coast and Island development of Ministry of Education, School of  
6 Geographic and Oceanographic Sciences, Nanjing University, Nanjing 210093, China;

7 2.Geology Department, University of Dayton, Ohio 45469-2364, USA;

8 \*Correspondence to: Hongxi Pang (hxpang@nju.edu.cn); Shugui Hou (shugui@nju.edu.cn)

9  
10 **Abstract.** In the Asian monsoon region, variations in the stable isotopic composition of  
11 speleothems have often been attributed to the “amount effect”. However, an increasing number  
12 of studies suggest that the “amount effect” in local precipitation is insignificant or even  
13 non-existent. To explore this issue further, we examined the variability of daily stable isotopic  
14 composition ( $\delta^{18}\text{O}$ ) in precipitation from September 2011 to November 2014 in Nanjing, East  
15 China. We found that  $\delta^{18}\text{O}$  in summer precipitation was not significantly correlated with local  
16 rainfall amount, but could be linked to changes in the location and rainout processes of  
17 precipitation source regions. Our findings suggest that the stable isotopes in summer  
18 precipitation could signal the location shift of precipitation source regions in the inter-tropical  
19 convergence zone (ITCZ) over the course of the monsoon season. As a result, changes in  
20 moisture source location and upstream rainout effect should be taken into account when  
21 interpreting the stable isotopic composition of speleothems in the Asian monsoon region. In  
22 addition, the temperature effect on isotopic variations in non-monsoonal precipitation should be

23 also involved because precipitation in the non-monsoon season accounts for about half of its  
24 annual precipitation.

25

## 26 **1 Introduction**

27 The “amount effect” refers to the observed negative correlation between the isotopic  
28 composition in precipitation and rainfall amount. It was first put forward by Dansgaard (1964),  
29 and is generally observed in low-latitude regions (Araguás-Araguás et al., 1998). Based on this  
30 relationship, stable isotopic records obtained from low-latitude regions are often used for  
31 paleohydroclimate reconstructions (Cruz et al., 2005, 2009; Partin et al., 2007; Tierney et al.,  
32 2008; Sano et al., 2012). However, some recent studies suggest that the “amount effect” is  
33 insignificant or even non-existent in low-latitude monsoon areas. For example, Conroy et al.  
34 (2013) found spatial and temporal examples of precipitation–isotope mismatches across the  
35 tropical Pacific, indicating that factors beyond the “amount effect” influence precipitation  
36 isotope variability. They compared 12 isotope-equipped global climate models to assess the  
37 distribution of simulated stable isotopic variability. Model simulations support observations in  
38 the western tropical Pacific, showing that monthly  $\delta^{18}\text{O}$  are correlated with large-scale, not local,  
39 precipitation (Conroy et al., 2013). Peng et al. (2010) also found no significant correlation  
40 between precipitation amount and  $\delta^{18}\text{O}$  values in the western Pacific monsoon region near  
41 Taiwan. They suggest that moisture sources of diverse air masses with different isotopic signals  
42 are the main factor controlling the precipitation isotopic characteristics. Breitenbach et al. (2010)  
43 observed no empirical amount effect at their study site in the monsoonal northeast India. They  
44 identified a strong trend towards lighter isotope values over the course of the summer monsoon,

45 with lowest  $\delta^{18}\text{O}$  and  $\delta\text{D}$  values in late monsoon season, with a temporal offset between the  
46 highest rainfall and the most negative  $\delta^{18}\text{O}$ . Other observations (Lawrence et al., 2004; Kurita et  
47 al., 2009) show that at marine island stations, even short-term (daily or event-based) isotopic  
48 variations are independent of local precipitation intensity, but linked to the rainout process in the  
49 surrounding regions. Some ice core studies also suggest that records of precipitation  $\delta^{18}\text{O}$  in ice  
50 cores of the Indian monsoon region do not match the local precipitation amount. For example,  
51 Pang et al. (2014) found a significant correlation between  $\delta^{18}\text{O}$  records from the East Rongbuk  
52 ice cores and summer monsoon rainfall along the southern slope of the Himalayas, whereas no  
53 significant correlation was found between the  $\delta^{18}\text{O}$  records and accumulation rates (an indicator  
54 of local precipitation). This suggests that summer monsoon precipitation  $\delta^{18}\text{O}$  over the high  
55 Himalayas is controlled by the upstream rainout over the entire southern slope of the Himalayas  
56 rather than local precipitation processes.

57 Stable oxygen isotopes in speleothems are widely used for paleoclimate reconstructions.  
58 Recently, stable oxygen isotopes measured in cave speleothems from China have received much  
59 attention: e.g., Hulu Cave (Wang et al., 2001), Dongge Cave (Yuan et al., 2004; Dykoski et al.,  
60 2005; Kelly et al., 2006), Sanbao Cave (Wang et al., 2008; Cheng et al., 2009), Heshang Cave  
61 (Hu et al., 2008), Wanxiang Cave (Zhang et al., 2008), Buddha Cave (Paulsen et al., 2003), and  
62 Dayu Cave (Tan et al., 2009) (Fig. 1). However, the interpretation of these stable isotope records  
63 in speleothems remains controversial. Some researchers used the stable isotope records from  
64 stalagmites in monsoonal east China as proxies for precipitation amount (Hu et al., 2008; Tan et  
65 al., 2009; Cai et al., 2010). Paulsen et al. (2003) showed that short-term (<10 years) variations in  
66  $\delta^{18}\text{O}$  in stalagmites from Buddha Cave reflect changes in precipitation amounts, but longer-term

67 (>50 years)  $\delta^{18}\text{O}$  variations indicate changes in air temperature. Other studies suggest that  $\delta^{18}\text{O}$   
68 indicates changes in the ratio of summer to winter precipitation, which they refer to as “monsoon  
69 intensity” (Wang et al., 2001; Yuan et al., 2004; Dykoski et al., 2005; Kelly et al., 2006; Wang et  
70 al., 2008; Zhang et al., 2008; Cheng et al., 2009). Dayem et al. (2010) reported that annual and  
71 rainy season precipitation totals in each of central China, south China, and east India have  
72 correlation length scales of  $\sim 500$  km, shorter than the distance between many speleothem records  
73 that share similar long-term time variations in  $\delta^{18}\text{O}$  values. Thus, the short correlation distances  
74 do not support the idea that apparently synchronous variations in  $\delta^{18}\text{O}$  values at widely spaced  
75 (>500 km) caves in China are due to variations in annual precipitation amounts. Most of the  
76 above-mentioned studies indicate that the variations of  $\delta^{18}\text{O}$  in speleothems from the Asian  
77 summer monsoon region are not controlled by the local precipitation amount.

78       Recent studies have revealed the importance of variability in moisture sources (Peng et al.,  
79 2010; Xie et al., 2011) and large-scale convective activities (Vimeux et al., 2011; Tremoy et al.,  
80 2012; Kurita, 2013; Moerman et al., 2013; [Lekshmy et al., 2014](#); [He et al., 2015](#)) in controlling  
81 precipitation  $\delta^{18}\text{O}$  in monsoon regions. Strong convection at source regions tends to produce  
82 more precipitation, causing heavy isotopes to preferentially condense from vapor, leading to  
83 lower values of downstream precipitation  $\delta^{18}\text{O}$ . In addition, the location of moisture source  
84 determines the distance that water vapor has to travel, hence affects the precipitation  $\delta^{18}\text{O}$ .  
85 Soderberg et al. (2013) found that the variability of the isotopic composition of individual rain  
86 events in central Kenya could be partly explained by the distance traveled of air mass over land.  
87 Therefore, the rainout effect at the water vapor source areas and upstream regions should have a  
88 significant influence on stable isotopes in precipitation in downstream regions ([Vuille et al.,](#)

89 2005).

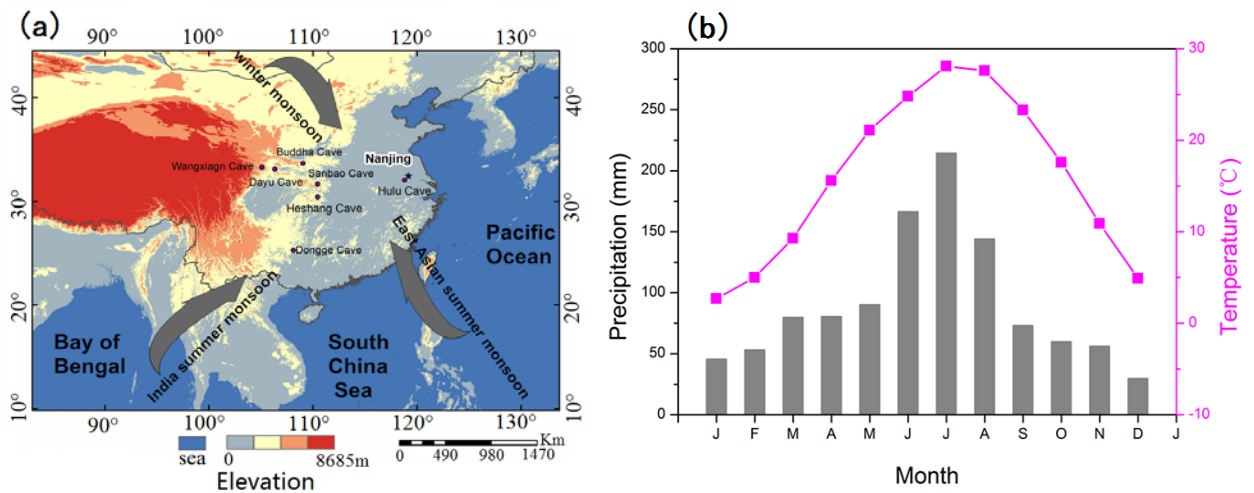
90 In the Asian monsoon regions, moisture sources for summer precipitation often lie in the  
91 strong convection areas within the inter-tropical convergence zone (ITCZ). The variability of  
92 ITCZ position and intensity could therefore affect precipitation  $\delta^{18}\text{O}$  in these regions. Using the  
93 outgoing longwave radiation (hereafter OLR) as a tracer for deep tropical convection (Wang et  
94 al., 1997), the ITCZ position and strength could be identified (Gu and Zhang, 2002). In the East  
95 Asia–West Pacific region, the onset of the Asian summer monsoon corresponds to the northward  
96 movement of the ITCZ to an area between  $5^{\circ}$ – $25^{\circ}\text{N}$  (Ding, 2007), and brings with it large  
97 amount of convective precipitation (Ananthkrishnan et al., 1981). In this study, we examined in  
98 detail how summer precipitation  $\delta^{18}\text{O}$  related to changes in the position and intensity of moisture  
99 sources within ITCZ, using the daily  $\delta^{18}\text{O}$  data at Nanjing in summer (June–September) during  
100 2012–2014, the daily OLR data, and relevant meteorological data. The daily OLR data are from  
101 the NCEP reanalysis data, provided by the NOAA/ORA/ESRL PSD, Boulder, Colorado, USA,  
102 from their Web site at <http://www.esrl.noaa.gov/psd>. According to long term monthly means of  
103 Nanjing precipitation for the years 1981-2010 from the China Meteorological Data Sharing  
104 Service System (<http://cdc.nmic.cn/home.do>), summer precipitation (June-September) accounts  
105 for 54.8% of its annual precipitation, indicating that the non-monsoonal precipitation (45.2%)  
106 (October-May) is also important. Therefore, factors controlling the isotopic variations in the  
107 non-monsoonal precipitation were also discussed, aiming for improving the interpretation of the  
108 oxygen isotopic records in speleothems in the Asian monsoon region.

109

110 **2 Study area**

111 **2.1 General atmospheric circulation**

112 Nanjing is located on the lower reaches of the Yangtze River, surrounded by low hilly  
113 terrain with an average altitude of 26 m (Fig. 1a). The mean annual air temperature is 16°C and  
114 the average annual precipitation is 1106 mm. Located close to the Tropic of Cancer, this area has  
115 a strong seasonal climate (Fig. 1b), with a distinct seasonal reversal of wind and alternation of  
116 dry and rainy periods. In the winter, the air masses over Nanjing mainly originate from the high  
117 pressure system over Mongolia in the North and West (Fig. 1a). In the summer, the city is under  
118 the influence of both the East Asian summer monsoon and the Indian summer monsoon (Fig. 1a).



119 Fig. 1. (a) Elevation map of China; the study site Nanjing is marked by a black star. Black dots  
120 indicate the cave locations mentioned in this study: Hulu, Dongge, Heshang, Sanbao, Wanxiang,  
121 Buddha, and Dayu. Grey arrows indicate the dominant circulation patterns over the region. (b)  
122 Monthly average temperature (T) and monthly average precipitation (P) for the years 1981–2010;  
123 data from the China Meteorological Data Sharing Service System.  
124

125  
126 **2.2 Intraseasonal variations in the Asian Summer Monsoon**

127 With the onset of the summer monsoon, the warm and moist air masses from the south

128 collide with cold northerly air masses in east China, forming a quasi-stationary rain belt known  
129 as Meiyu. The weather systems developed at the Meiyu front provide the majority of summer  
130 precipitation in this region, with the enhanced moisture transport from the South China Sea and  
131 the Bay of Bengal (Ding, 1992). The Meiyu system also includes the Baiu in Japan (Saito, 1995)  
132 and the Changma in Korea (Oh et al., 1997). Meiyu starts in southern China between April and  
133 May, moving to the middle part of eastern China (Yangtze and Huai He River Basins) in May  
134 and July, and to northern China in July and August, bringing with it consistent rainfall. Baiu  
135 occurs from mid-June to mid-July in Japan (Saito, 1995), and Changma takes place from the end  
136 of June to the end of July when the rain belt shifts northward to Korea (Oh et al., 1997). The  
137 retreat of the Asian summer monsoon is observed earliest in East Asia, and occurs very rapidly,  
138 taking only a month or less to retreat from northern to southern China. In early September, the  
139 leading edge of the summer monsoon quickly withdraws southward to the northern part of the  
140 **South China Sea** and remains there, marking the end of the summer monsoon in East Asia (Ding,  
141 1992; Ding, 2007).

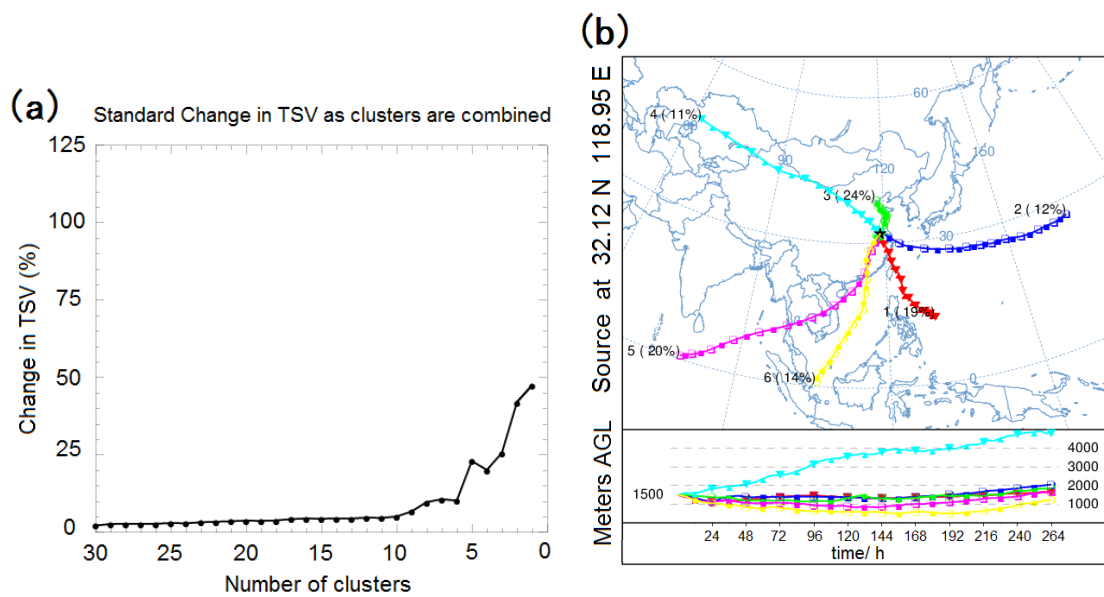
142

### 143 **2.3 Moisture sources of summer precipitation**

144 To determine the probable source regions of the air masses influencing our study area, we  
145 generated backward trajectories based on the Hybrid Single-Particle Lagrangian Integrated  
146 Trajectories (HYSPLIT) of the Air Resources Laboratory of the US National Oceanic and  
147 Atmospheric Administration, based on the data generated by the Global Data Assimilation  
148 System (GDAS) (<ftp://arlftp.arlhq.noaa.gov/pub/archives/gdas1>). Although backward trajectory  
149 analysis only reflects the synoptic situation and is only an approximation of the general origin of

150 an air mass, this approach has been widely used in studies of moisture transport (Brimelow et al.,  
 151 2005; Perry et al., 2007; Sodemann et al., 2009; Drumond et al., 2011). In our study, the vapor  
 152 source trajectory was simulated for each summer precipitation event from June to September,  
 153 and cluster analysis was applied to the trajectories. The moisture transport paths were identified  
 154 using the HYSPLIT back trajectory model combined with NCEP reanalysis at 12-h time steps  
 155 back to 11 d at 1500 m AGL (above ground level) (about 850 hPa), as water vapor transport is  
 156 usually concentrated in the middle and lower troposphere (Bershaw et al., 2012). The total spatial  
 157 variance (TSV) (Fig. 2a) was used to identify the optimum number of clusters. Rapid growth in  
 158 TSV occurred when the number of clusters fell below six, therefore six clusters were retained as  
 159 the final simulated cluster trajectories.

160 The simulation suggests that in summer, Nanjing was dominated by the influence of several  
 161 major moisture sources: the Bay of Bengal, the South China Sea, the western Pacific, and the  
 162 northern inland areas (Fig. 2b).



163  
 164 Fig. 2. (a) Change in TSV (total spatial variance) as clusters are combined, and (b) Spatial  
 165 distribution of water vapor pathways. The percentage shows the frequency of each clustered

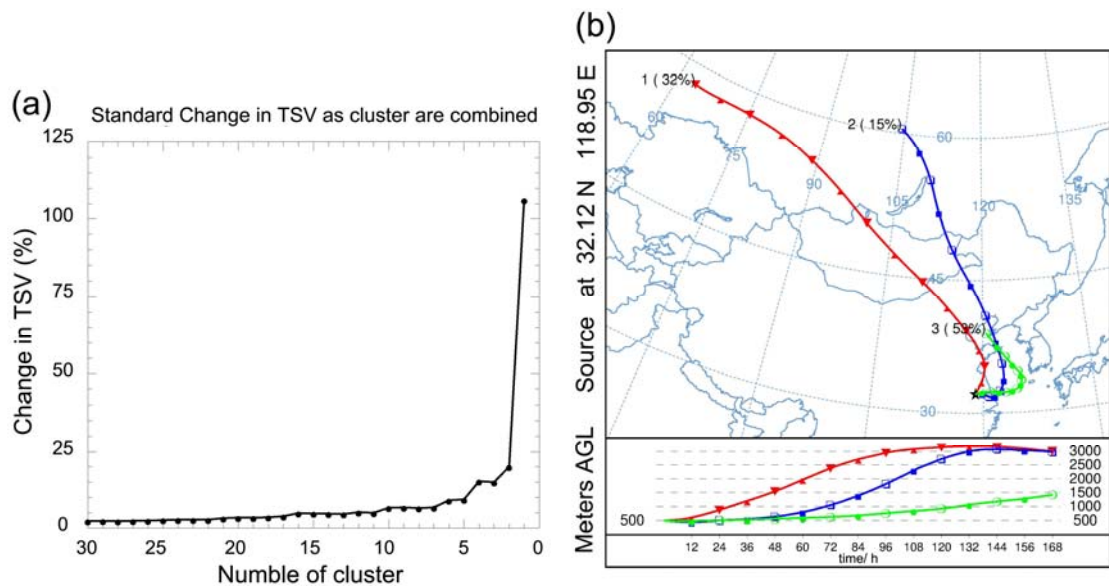


166 backward trajectory in summer season.

167

## 168 2.4 Moisture sources of non-monsoonal precipitation

169 The vapor source trajectory for each non-monsoonal precipitation event from October to  
170 May was also simulated by the HYSPLIT model using the same method used for summer  
171 precipitation. The moisture transport paths back to 7d at 500 m AGL were determined by the  
172 model because of the stronger wind speed and relatively lower height of precipitation  
173 condensation in the non-monsoon season. The simulated trajectories are presented in Fig. 3. The  
174 simulation suggests that in the non-monsoon season, Nanjing was dominated by two major  
175 moisture sources: the remote inland of the Eurasia and the China offshore seas (the Yellow Sea  
176 and the Bohai Sea) (Fig. 3).



177

178 Fig. 3. (a) Change in TSV (total spatial variance) as clusters are combined, and (b) Spatial  
179 distribution of water vapor pathways. The percentage shows the frequency of each clustered  
180 backward trajectory in the non-monsoon season.

181

### 182 **3 Sampling and isotope measurements**

183 Using a deep open-mouthed container, precipitation samples were collected on days with  
184 precipitation greater than 0.1 mm from September 2011 to November 2014 with the exception of  
185 January-April 2013. Immediately after collection, the samples were poured into 100 mL  
186 polyethylene bottles and sealed tightly for storage in a freezer.

187 The  $\delta^{18}\text{O}$  and  $\delta\text{D}$  of these samples were **simultaneously** measured using a Picarro L2120-i  
188 wavelength scanned-cavity ring down spectroscopy (WS-CRDS) system at the Key Laboratory  
189 of Coast and Island Development of the Ministry of Education, School of Geographic and  
190 Oceanographic Sciences, Nanjing University, China.

191 The stable isotopic ratio was calculated as:

$$192 \quad \delta = \left[ \frac{R_{\text{sample}}}{R_{\text{reference}}} - 1 \right] \times 1000 \text{‰}$$

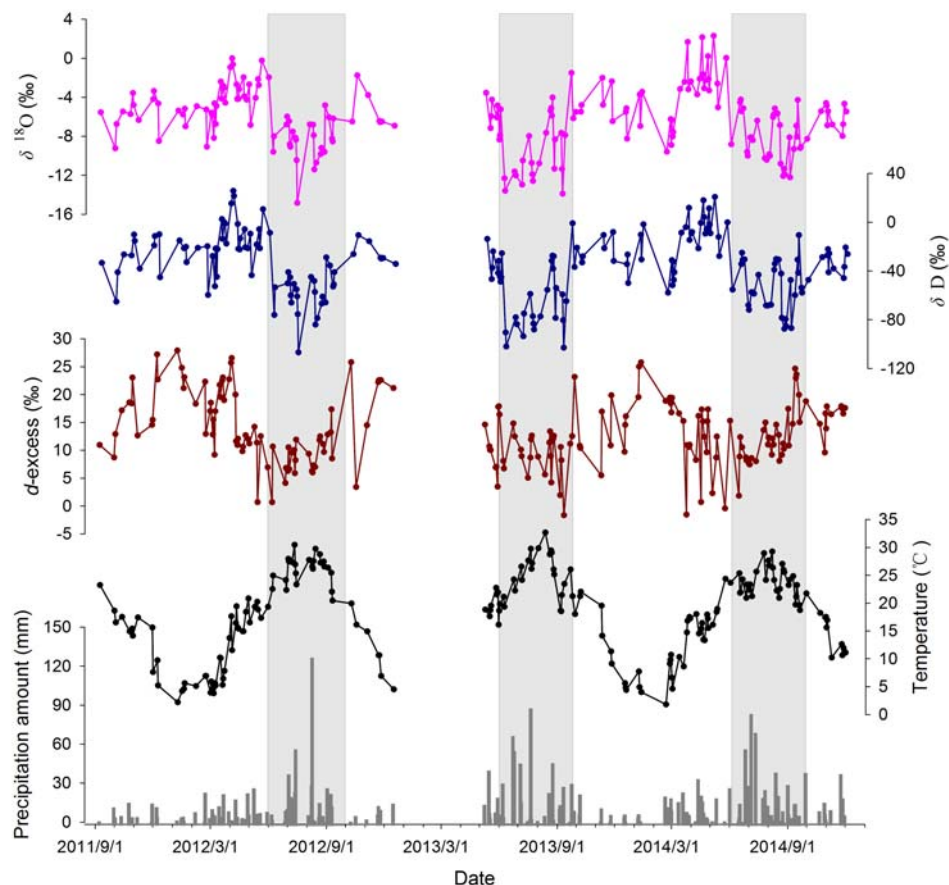
193 where  $R$  is the ratio of the composition of the heavier to lighter isotopes in water ( $^{18}\text{O}/^{16}\text{O}$  for  
194  $\delta^{18}\text{O}$ , or D/H for  $\delta\text{D}$ ), and the reference is the Vienna Standard Mean Ocean Water standard.  
195 Each sample was measured eight times. The first five measurements were discarded in order to  
196 eliminate the effect of memory. **The average of the last three measurements was calibrated based**  
197 **on the linear regression between the known isotopic values of our three internal water standards**  
198 **and their measured values. The calibrated values of samples were taken as the test results. The**  
199 **analytical uncertainty is less than 0.1‰ for  $\delta^{18}\text{O}$  and 0.5‰ for  $\delta\text{D}$ . A quadratic error for d-excess**  
200 **is less than 1.0‰, estimated by the uncertainties of  $\delta^{18}\text{O}$  and  $\delta\text{D}$ .**

201

## 202 **4 Results**

### 203 **4.1 Seasonal variations of stable isotopes in precipitation**

204 Temporal variations of daily precipitation stable isotopes ( $\delta^{18}\text{O}$ ,  $\delta\text{D}$  and d-excess),  
 205 precipitation amount, and surface air temperature in Nanjing during the observation period are  
 206 presented in Fig. 4. The isotopic data exhibits significant seasonal variations, with low values of  
 207 the  $\delta^{18}\text{O}$ ,  $\delta\text{D}$  and d-excess in the summer monsoon season and high values in the non-monsoon  
 208 season. In detail, the  $\delta^{18}\text{O}$  values in the summer monsoon season (the non-monsoon season) vary  
 209 from -14.8‰ to -1.5‰ (-9.5‰ to 2.3‰), from -106.0‰ to -0.3‰ (-59.0‰ to 26.2‰) for  $\delta\text{D}$ ,  
 210 and from -1.4‰ to 24.8‰ (-1.3‰ to 28.1‰) for d-excess. The mean weighted-precipitation  $\delta^{18}\text{O}$   
 211 in the summer monsoon season (the non-monsoon season) is -9.1‰ (-4.9‰), -61.8‰ (-23.4‰)  
 212 for  $\delta\text{D}$ , and 10.9‰ (15.5‰) for d-excess.



213

214 Fig. 4. Temporal variations of daily precipitation  $\delta^{18}\text{O}$ ,  $\delta\text{D}$ , d-excess, precipitation amount, and  
 215 surface air temperature in Nanjing from September 2011 to November 2014. The shaded bars

216 represent the summer monsoon seasons (June to September). Note the missing data from January  
217 to April 2013. The daily precipitation amount and surface air temperature data were from the  
218 China Meteorological Data Sharing Service System.

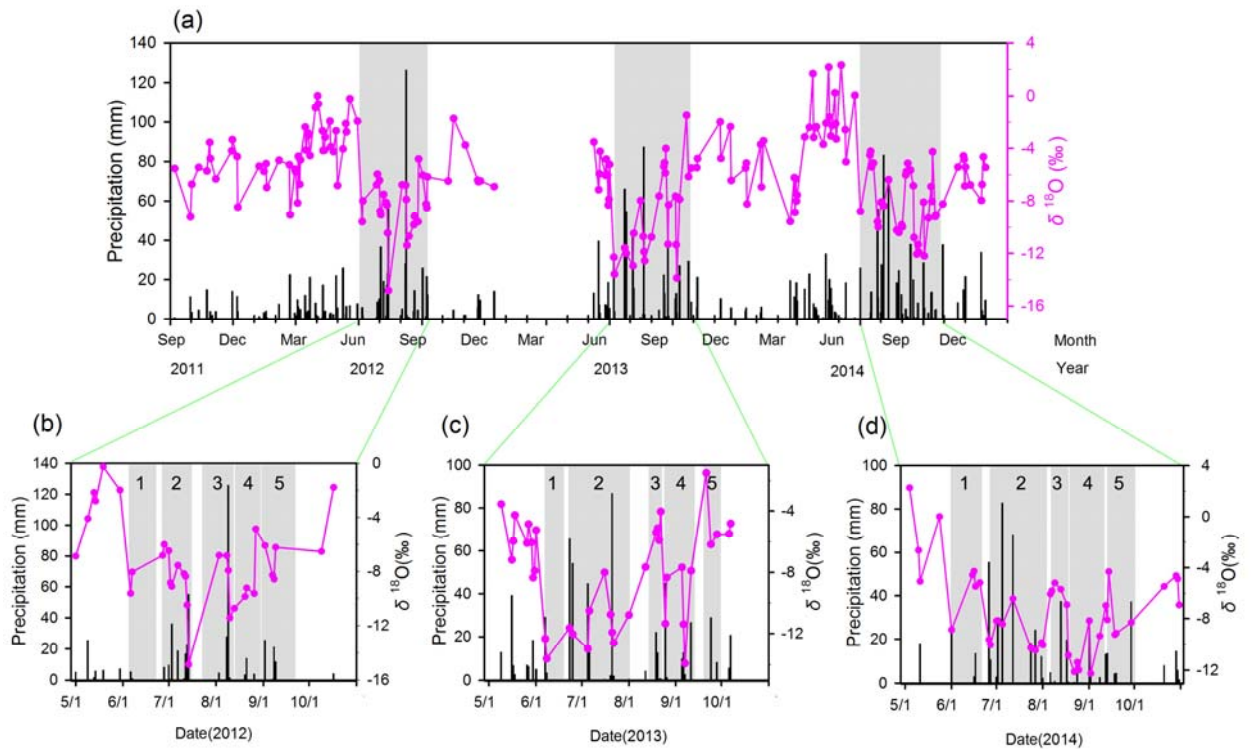
219

#### 220 **4.2 $\delta^{18}\text{O}$ variations in summer precipitation**

221 In 2012, after a sudden decrease on June 6, the precipitation  $\delta^{18}\text{O}$  remained low, reaching a  
222 minimum (-14.8‰) on July 14. The  $\delta^{18}\text{O}$  values increased in early August, and decreased again  
223 in late August. In early September,  $\delta^{18}\text{O}$  in precipitation became enriched (Fig. 5b). In 2013,  
224 precipitation  $\delta^{18}\text{O}$  decreased suddenly on June 7, then increased slowly until it peaked (-4.0‰)  
225 on August 22. The stable isotope composition was depleted in late August and reached a  
226 minimum (-13.8‰) on September 7. In late September,  $\delta^{18}\text{O}$  in precipitation was enriched (Fig.  
227 5c). In 2014,  $\delta^{18}\text{O}$  in precipitation decreased on June 1 and slightly increased afterward until it  
228 was depleted again in July. It started to increase in early August. From late August to early  
229 September,  $\delta^{18}\text{O}$  in precipitation remained depleted, but became enriched since late September  
230 (Fig. 5d).

231 We divided the summer into 5 distinct stages (Figure 5), based on the temporal patterns  
232  $\delta^{18}\text{O}$  variations, together with the intraseasonal variations in the Asian summer monsoon and  
233 Meiyu (see section 2.2). Stage 1 started with the sudden decrease in  $\delta^{18}\text{O}$  in early June, which is  
234 generally considered as an indicator for the onset of the summer monsoon (e.g., Tian et al., 2001;  
235 Vuille et al., 2005; Yang et al., 2012). Stage 2 covered the Meiyu period. The start dates of Meiyu  
236 in 2012–2014 were June 26, June 23, and June 25 respectively, based on the observations by the  
237 Jiangsu Provincial Meteorological Bureau. Stage 3 was characterized by relatively high

238 precipitation  $\delta^{18}\text{O}$ , whereas in stage 4,  $\delta^{18}\text{O}$  remained low. Stage 5 marked the return of  $\delta^{18}\text{O}$   
 239 values to enriched state. The 5 stages were delineated in Figure 5(b)-(d).



240  
 241 Fig. 5. (a) Temporal variation of daily precipitation  $\delta^{18}\text{O}$  and precipitation amount (P) from  
 242 September 2011 to November 2014. The daily precipitation data were from the China  
 243 Meteorological Data Sharing Service System. Note the missing data for  $\delta^{18}\text{O}$  from January to  
 244 April 2013. (b)–(d): Temporal variations in daily precipitation  $\delta^{18}\text{O}$  and local precipitation  
 245 amount from May to October in 2012 (b), 2013 (c), 2014 (d). The shaded bars represent different  
 246 stages.

247 In (b) for 2012, stage 1: June 3 - June 20; stage 2: June 27 - July 14; stage 3: July 20 - August 9;  
 248 stage 4: August 10 - August 26; and stage 5: August 27 - September 20.

249 In (c) for 2013, stage 1: June 7 - June 20; stage 2: June 23 - August 1; stage 3: August 12 -  
 250 August 22; stage 4: August 25 - September 11; and stage 5: September 20 - September 30.

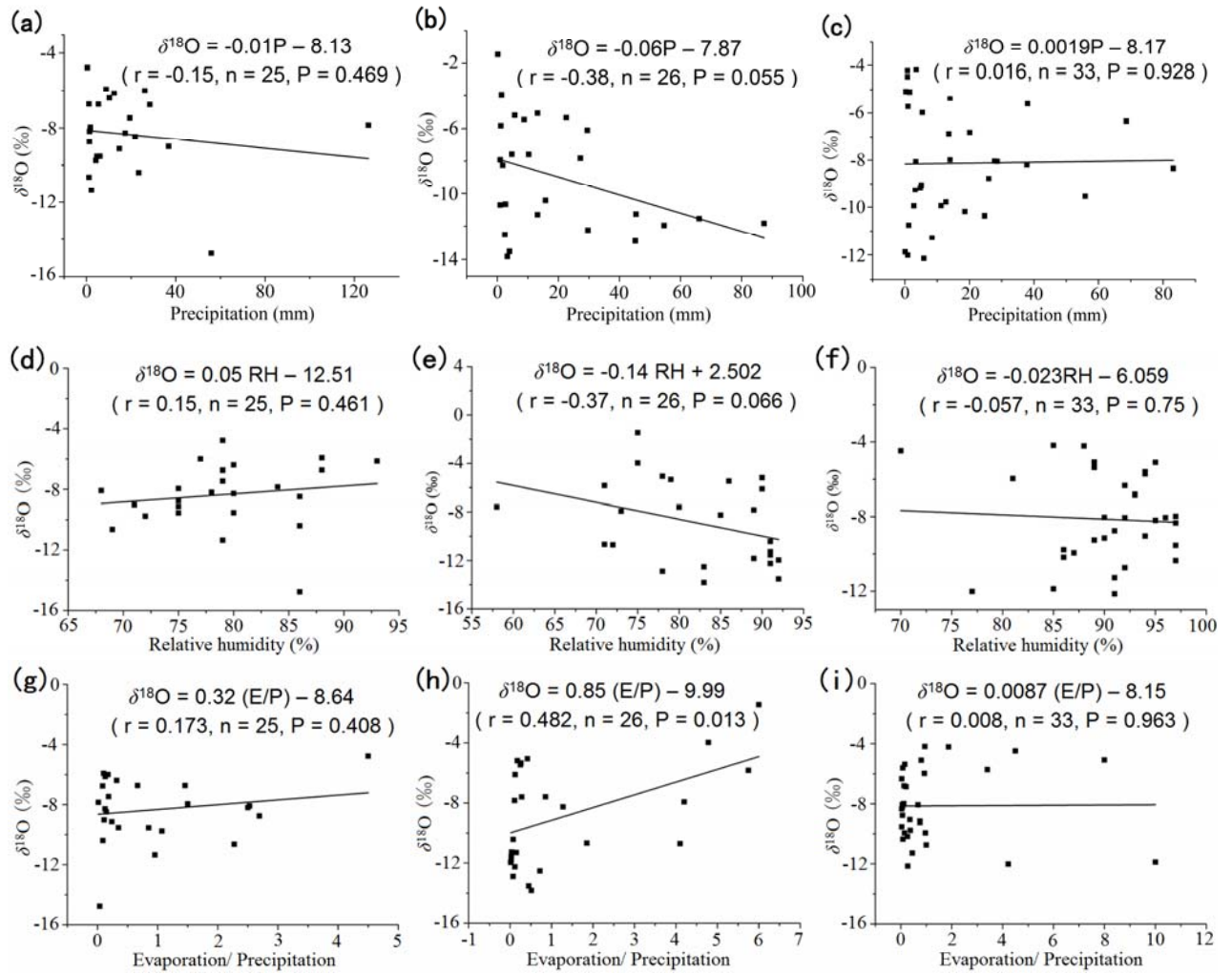
251 In (d) for 2014, stage 1: June 1 - June 20; stage 2: June 26 - August 1; stage 3: August 6 - August

252 17; stage 4: August 18 - September 8; and stage 5: September 12 - September 30.

253

#### 254 **4.3 The amount effect of $\delta^{18}\text{O}$ in summer precipitation**

255 The amount effect refers to the observed negative correlation between precipitation isotopic  
256 composition and precipitation amount (Dansgaard, 1964). The most discussed mechanism for the  
257 amount effect is that high precipitation rates increase relative humidity, hence decrease  
258 evaporation. As evaporation serves to enrich heavy isotopes, its reduction leads to more depleted  
259 precipitation isotopic signatures. Moreover, high relative humidity also inhibits re-evaporation of  
260 local surface water (lakes and streams) to feed back into the precipitation. As local surface water  
261 is usually more enriched in heavy isotopes, its diminished input also leads to more depleted  
262 precipitation isotopic composition. Here we investigated if the amount effect could be clearly  
263 observed from our data. We performed separate correlation analyses between precipitation  $\delta^{18}\text{O}$   
264 and precipitation amount, relative humidity and the evaporation ratio defined as evaporation  
265 divided by precipitation (E/P) (Fig. 6). There was a weak negative correlation between  
266 precipitation  $\delta^{18}\text{O}$  and precipitation amount in 2013 (Fig. 6b). In addition, precipitation  $\delta^{18}\text{O}$   
267 became more depleted with increased relative humidity (Fig. 6e) and decreased  
268 evaporation/precipitation ratio (Fig. 6h). This seems to suggest that the amount effect was  
269 present in the 2013 data. However, no significant correlation was observed in 2012 and 2014  
270 (Fig. 6a, c).



271

272

273

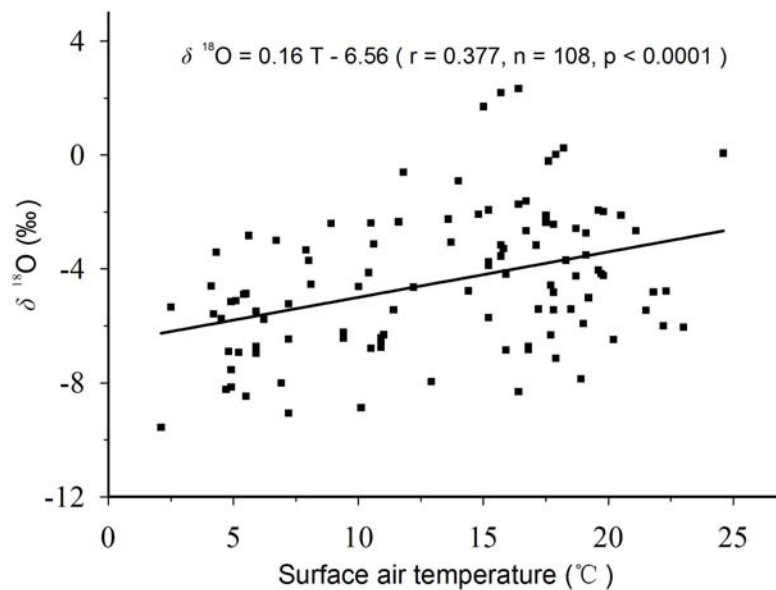
274 Fig. 6. This figure shows: (1) correlation between  $\delta^{18}\text{O}$  and precipitation amount in Nanjing from  
 275 June to September for 2012 (a), 2013 (b) and 2014 (c); (2) correlation between  $\delta^{18}\text{O}$  and relative  
 276 humidity in Nanjing from June to September for 2012 (d), 2013 (e) and 2014 (f); (3) correlation  
 277 between  $\delta^{18}\text{O}$  and evaporation/precipitation in Nanjing from June to September for 2012 (g),  
 278 2013 (h) and 2014 (i). Linear regression lines, correlation coefficient  $r$  and  $p$ -values are also  
 279 shown.

280

#### 281 4.4 The temperature effect of $\delta^{18}\text{O}$ in non-monsoonal precipitation

282 Although the temperature effect of stable isotopes in precipitation in southeast Asia is often  
 283 damped or even reverse due to the summer monsoon influence (Araguas-Araguas et al., 1998),

284 the temperature effect generally exists in the non-monsoonal season due to the winter monsoon  
285 influence. As expected, the daily precipitation  $\delta^{18}\text{O}$  was positively correlated with surface air  
286 temperature in the non-monsoon seasons of the observation period, with a linear T- $\delta^{18}\text{O}$   
287 relationship:  $\delta^{18}\text{O} = 0.16 T - 6.56$  (Fig. 7).



288

289 Fig. 7. Correlation between daily precipitation  $\delta^{18}\text{O}$  and surface air temperature (T) in Nanjing in  
290 the non-monsoon seasons of the observation period.

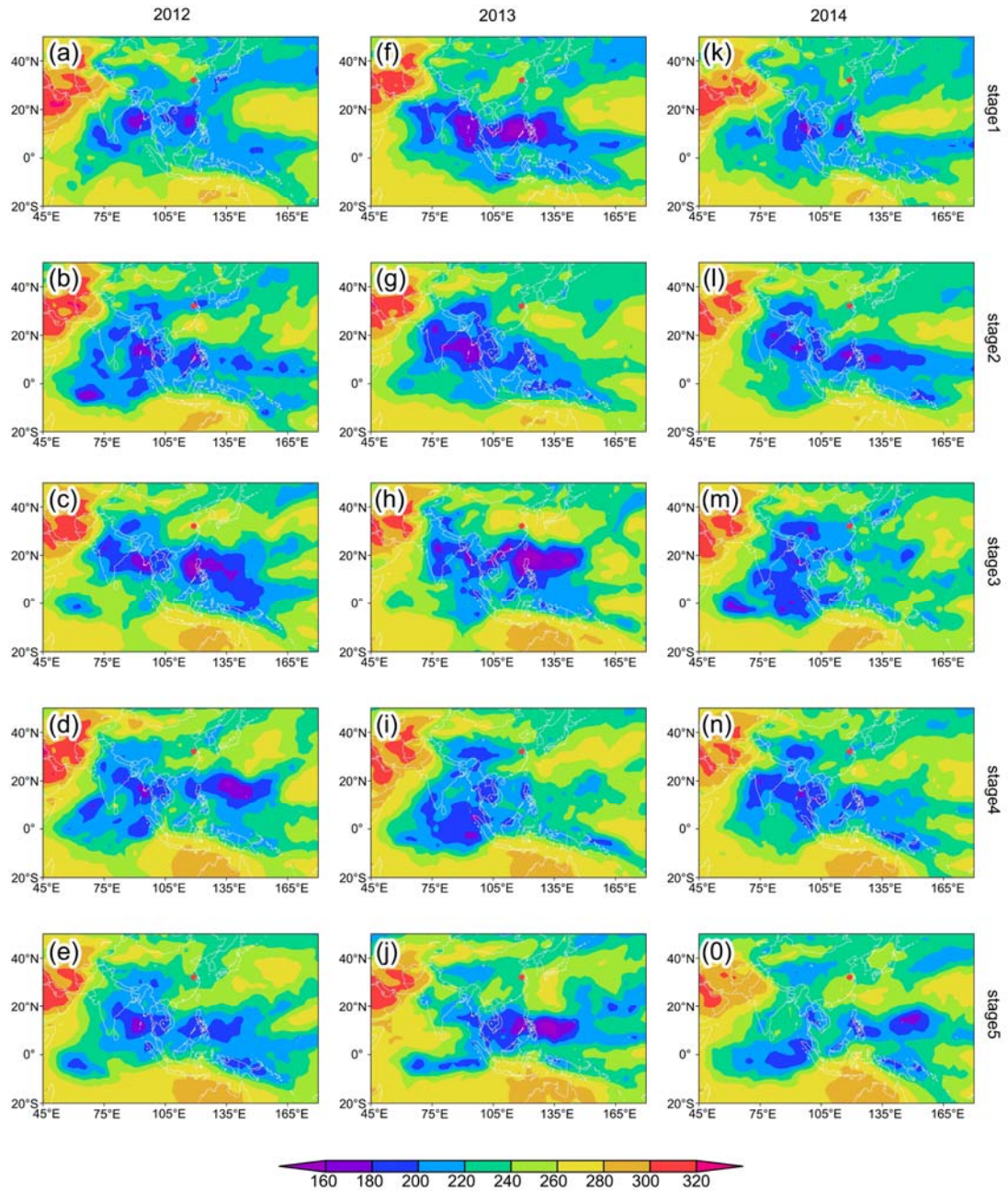
291

## 292 5 Discussion

293 The ITCZ region is an important moisture source for precipitation in general, and for  
294 monsoon precipitation in particular. Therefore, the monsoon is often considered as a  
295 manifestation of the intraseasonal migration of the ITCZ (Gadgil, 2003). To explore the possible  
296 influence of ITCZ intensity and position on  $\delta^{18}\text{O}$  in summer precipitation in Nanjing, a  
297 composite analysis of OLR was performed for each stage (Fig. 8). Low OLR values correspond  
298 to cold and high clouds associated with enhanced convection, and a negative relationship is  
299 generally observed between OLR and convection intensity (Wang et al., 1997). Therefore, a



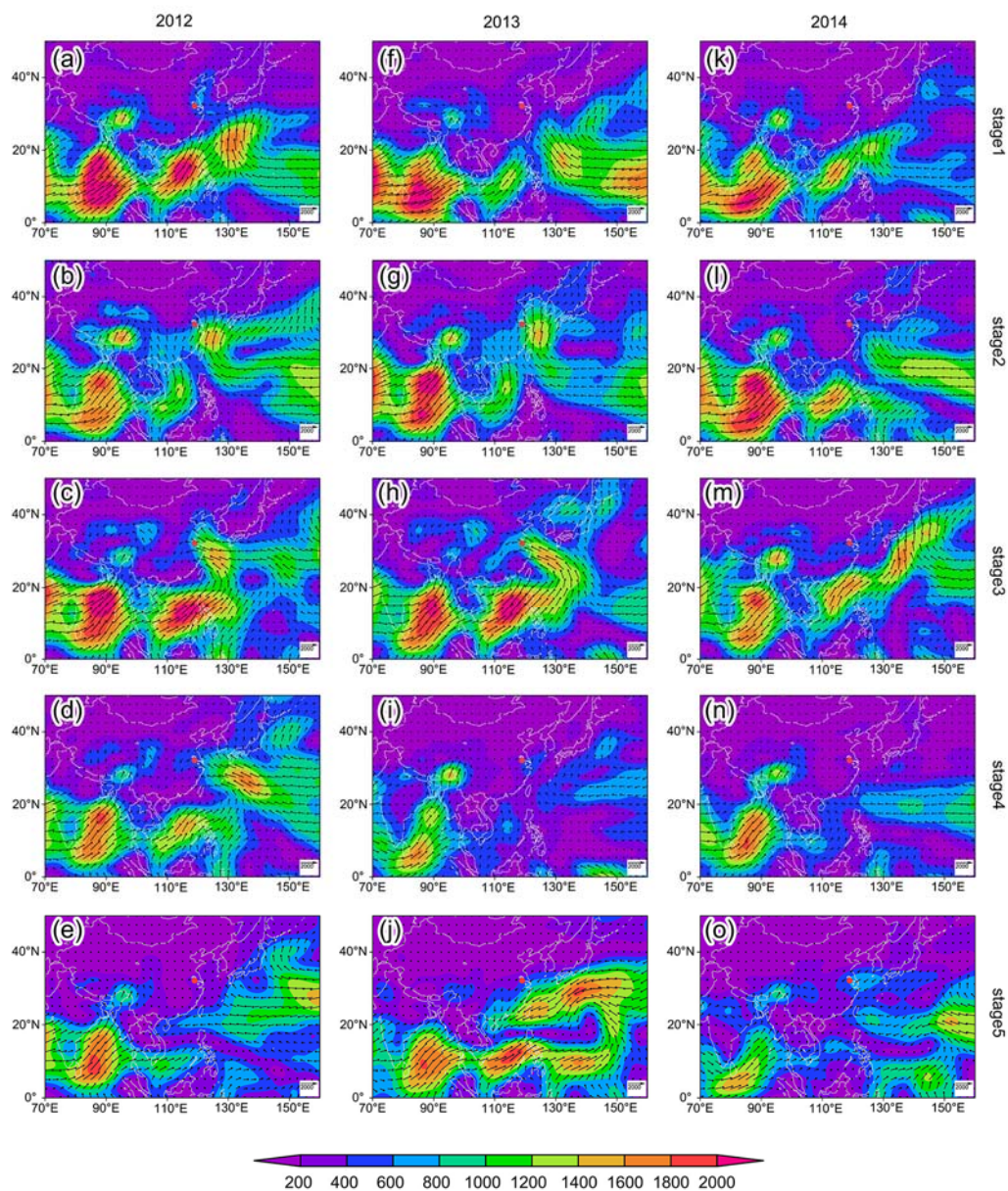
300 composite analysis of OLR could help establish the location and intensity of deep convections  
301 associated with ITCZ, which serve as moisture sources for the monsoon precipitation in Nanjing.  
302 It was also necessary to establish the moisture transport for each stage in order to link the source  
303 regions with our study area and determine the distance, as both could potentially influence the  
304 precipitation  $\delta^{18}\text{O}$ . To achieve this, we calculated the vertically integrated mean water vapor  
305 transport for each stage, using the daily NCEP/NCAR reanalysis data (Fig. 9). This was  
306 calculated as the horizontal wind field (zonal and meridional winds) multiplied by specific  
307 humidity, which was then integrated from surface to 300 hPa level.



308

309 Fig. 8. Composite results for average OLR ( $\text{W m}^{-2}$ ) for stages 1 to 5. The convective activity is  
 310 indicated by low values in OLR. Daily OLR data at  $2.5^\circ \times 2.5^\circ$  resolution were used  
 311 (<http://www.esrl.noaa.gov/psd>). The study site of Nanjing is marked by a red dot. (a)–(e): stages  
 312 1 to 5 in 2012; (f)–(j): stages 1 to 5 in 2013; (k)–(o): stages 1 to 5 in 2014.

313



314

315 Fig. 9. Vertically integrated mean water vapor transport ( $\text{g cm}^{-1} \text{s}^{-1}$ ). Different colors indicate the  
 316 magnitude of the moisture flux vector. The study site of Nanjing is marked by a red dot. (a)–(e)  
 317 standing for stages 1 to 5 in 2012; (f)–(j) for stages 1 to 5 in 2013; (k)–(o) for stages 1 to 5 in  
 318 2014.

319

320 In stage 1, the abrupt decrease of  $\delta^{18}\text{O}$  indicated the onset of the Asian summer monsoon,  
 321 with strong ITCZ convections in the Bay of Bengal and the South China Sea (Fig. 8a, f, k), and

322 **the delivery** of moisture from both regions (Fig. 9a, f, k). The isotope fractionation that occurred  
323 during the strong convection and the transport process lightened the stable isotopes in water  
324 vapor, resulting in the abrupt decrease of  $\delta^{18}\text{O}$  in precipitation in Nanjing.

325 In stage 2, the ITCZ intensity and location in 2012 did not change significantly from stage 1  
326 (Fig. 8b), and  $\delta^{18}\text{O}$  remained low. The extreme negative  $\delta^{18}\text{O}$  on July 14 was due to the  
327 continuous local rainfall from July 12 to 14, further depleting  $\delta^{18}\text{O}$  in precipitation. In 2013, the  
328 ITCZ intensity did not change much in the **Bay of Bengal**, but decreased significantly in the  
329 **South China Sea** and the low-latitude western Pacific Ocean (Fig. 8g). Weak convection reduced  
330 the rainout effect, and hence increased  $\delta^{18}\text{O}$  in precipitation. In 2014 the ITCZ intensity  
331 increased in the **South China Sea** and the low-latitude western Pacific Ocean, but it did not  
332 change significantly in the **Bay of Bengal** (Fig. 8l). At this stage, as the meridional water vapor  
333 transport to the north from the **South China Sea** increased (Fig. 9b, g, l), changes in convective  
334 activity in the **South China Sea** had a stronger influence on  $\delta^{18}\text{O}$  in study area precipitation.  
335 Strong convection in the **South China Sea** enhanced rainout effect, resulting in depleted  $\delta^{18}\text{O}$  in  
336 precipitation in Nanjing.

337 In stage 3, the ITCZ intensity decreased in the **Bay of Bengal** in both 2012 and 2013, but  
338 increased in the **South China Sea** and the low-latitude western Pacific Ocean. The center of  
339 strong convection propagated northward (Fig. 8c, h). Water vapor mainly originated from the  
340 **South China Sea** and the low-latitude western Pacific Ocean (Fig. 9c, h) for this stage. The  
341 relatively shorter transport distance resulted in higher  $\delta^{18}\text{O}$  values in precipitation. In 2014, the  
342 ITCZ intensity was relatively low in the **South China Sea** and the low-latitude western Pacific  
343 Ocean (Fig. 8m). The water vapor came mainly from the adjacent seas (Fig. 8m). As a result, the

344 relatively weak convection in the area and short transport distance enriched  $\delta^{18}\text{O}$  in precipitation  
345 in Nanjing.

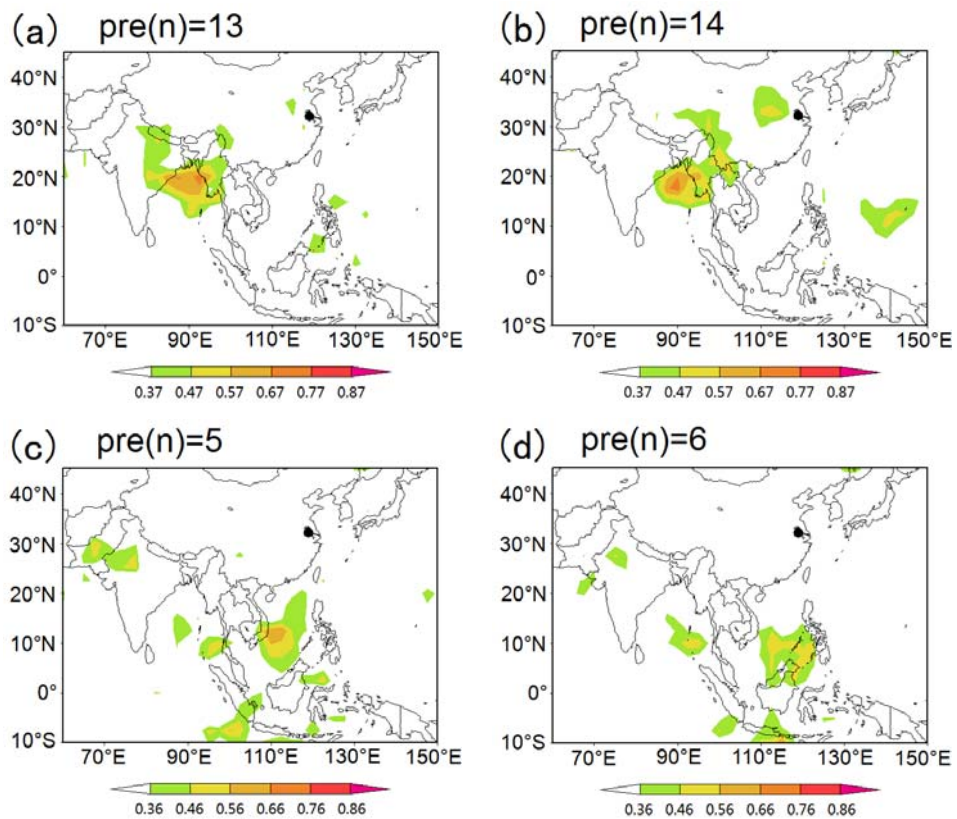
346 Stage 4 covered the late monsoon season. In 2012, in addition to increased convection  
347 strength in the west Pacific Ocean, the strong convective center also moved eastward, increasing  
348 the water transport distance to Nanjing. Both of these changes acted to deplete  $\delta^{18}\text{O}$  in  
349 precipitation. Moreover, the moisture transport suggested that vapor from the **Bay of Bengal** was  
350 also transported to Nanjing (Fig. 9d). The strong convection in the **Bay of Bengal** and its long  
351 distance from the study site contributed to further deplete  $\delta^{18}\text{O}$  in precipitation. In 2013 and 2014,  
352 the ITCZ intensity in the **South China Sea** and the western Pacific was relatively weak. However,  
353 both the moisture transport from the **Bay of Bengal** (Fig. 9i, n) and the convective activity in the  
354 **Bay of Bengal** was strong (Fig. 8i, n). In addition, the strong convective center in the **Bay of**  
355 **Bengal** moves southward in stage 4 of 2013 (Fig. 8i) resulting in longer distance from Nanjing.  
356 The combination of these factors depleted the isotopic composition of precipitation in this stage  
357 for both 2013 and 2014. The time series of  $\delta^{18}\text{O}$  in precipitation showed a clear trend of  
358 decreasing  $\delta^{18}\text{O}$ -values during the late monsoon period, while rainfall peaked earlier in the  
359 season. The depleted  $\delta^{18}\text{O}$  values in late monsoon season were also observed in the other  
360 monsoon areas. Pang et al. (2006) suggested that the low  $\delta^{18}\text{O}$  values were caused by the  
361 recycling of monsoon precipitation in late monsoon season. Breitenbach et al. (2010), on the  
362 other hand, argued that the **Bay of Bengal** freshwater plume, consisted of isotopically depleted  
363 rain water and snow melt water, diluted the **Bay of Bengal** surface water  $\delta^{18}\text{O}$  pool in late  
364 monsoon season. This contributed to the depleted  $\delta^{18}\text{O}$  in precipitation. Our results suggest that  
365 the depleted precipitation  $\delta^{18}\text{O}$  in the late monsoon season could result from the combination of

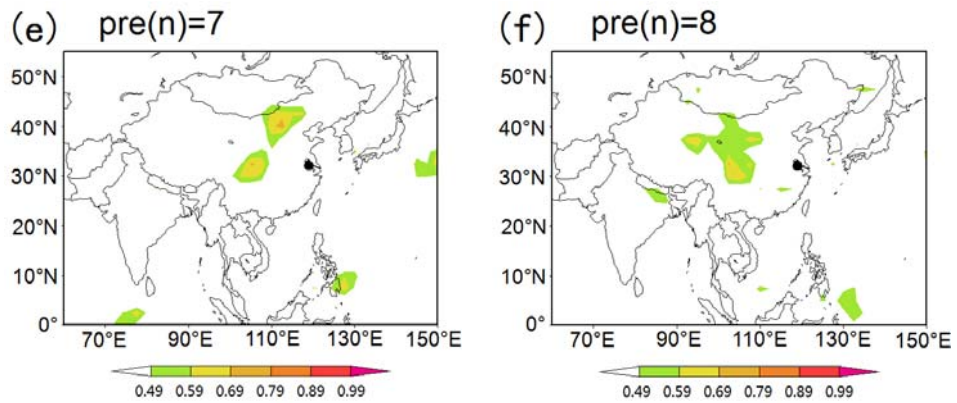
366 increased convective activities and transport distance due to the retreat of the ITCZ southward in  
367 the **Bay of Bengal**.

368 In stage 5, the Asian summer monsoon retreated and water vapor from the inland areas with  
369 a high stable isotopic composition was transported to Nanjing (Fig. 9e, j, o), enriching the  $\delta^{18}\text{O}$   
370 in precipitation. It is worth noting that the ITCZ intensity in the **South China Sea** and the  
371 low-latitude western Pacific Ocean strengthened in stage 5 of 2013 because of the super Typhoon  
372 Usagi. However, Nanjing was not affected due to its location at the edge of the Typhoon. At the  
373 time, the moisture in Nanjing came mainly from the northern inland areas and the adjacent seas  
374 in the northeast (Fig. 9e, j, o). Therefore, the stable isotopic composition of precipitation  
375 remained enriched.

376 The above observations seemed to suggest a close relationship between precipitation  $\delta^{18}\text{O}$   
377 and the convective activity in the moisture source regions. In order to further explore this  
378 relationship quantitatively, we performed a time-lagged spatial correlation analysis between  
379 precipitation  $\delta^{18}\text{O}$  in Nanjing and the daily OLR time series. Results are shown in Fig. 10.  
380 Several patterns emerged from this analysis. For stage 1 and 4, there was a **strongest** positive  
381 correlation between  $\delta^{18}\text{O}$  and OLR in the **Bay of Bengal** at 13 and 14 days before the rainfall  
382 (Fig. 10a, b). This supports the conclusion of previous studies that convective processes could  
383 have integrated impacts on water vapor over several days preceding precipitation events (Tremoy  
384 et al., 2012; Gao et al., 2013). For stage 2, our analysis showed a **strongest** positive correlation  
385 between  $\delta^{18}\text{O}$  and the OLR in the **South China Sea** at 5 and 6 days preceding the rainfall (Fig.  
386 10c, d). This confirms the significant influence of convective intensity in the **South China Sea** on  
387  $\delta^{18}\text{O}$  in precipitation in Nanjing at stage 2. As this stage covered the Meiyu period, this result is

388 largely in agreement with previous studies, which indicate that moisture for Meiyu precipitation  
 389 mainly comes from the **South China Sea** (Simmonds et al., 1999; Ding et al., 2007). For stage 5,  
 390 the **strongest** positive correlation was observed between daily  $\delta^{18}\text{O}$  in precipitation and OLR in  
 391 the inland areas to the north and west at 7 and 8 days before the rainfall (Fig. 10e, f), suggesting  
 392 that inland vapor contributed to  $\delta^{18}\text{O}$  in precipitation after the monsoon withdrew. However, no  
 393 significant correlation between  $\delta^{18}\text{O}$  and OLR was found for stage 3. This could partially  
 394 attributed to the shift of ITCZ location northward and eastward in 2012 and 2013 (Fig. 8c, h),  
 395 reducing the vapor transport distance (Fig. 9c, h). This could have played a more important role  
 396 in determining the  $\delta^{18}\text{O}$  values in precipitation in Nanjing than convective intensity.





399

400 Fig. 10. Spatial correlation between daily  $\delta^{18}\text{O}$  in precipitation and OLR at  $n$  days prior to the  
 401 rainfall date: Spatial correlation between  $\delta^{18}\text{O}$  in precipitation and OLR at 13 days (a) and 14  
 402 days (b) prior to the rainfall date for stages 1 and 4; Spatial correlation between  $\delta^{18}\text{O}$  in  
 403 precipitation and OLR at 5 days (c) and 6 days (d) prior to the rainfall date for stage 2; Spatial  
 404 correlation between  $\delta^{18}\text{O}$  in precipitation and OLR at 7 days (e) and 8 days (f) prior to the  
 405 rainfall date for stage 5. For all maps, only areas with correlations significant at 0.05 level are  
 406 shown. The study site Nanjing is marked with a black dot.

407

408 Our results suggest that the upstream convective activity over the tropical regions of the Bay  
 409 of Bengal, the South China Sea and the western Pacific has an important impact on the isotopic  
 410 composition of summer precipitation in Nanjing. Strong distillation processes during intense  
 411 convective activity would increase the rainout of heavy isotopes upstream, hence deplete the  
 412 isotopic composition in precipitation downstream, and vice versa. Therefore, the isotopic  
 413 composition in summer precipitation downstream of the moisture sources in the tropics could be  
 414 determined mainly by changes of the isotopic composition of atmospheric vapor in the upstream  
 415 source region rather than the precipitation amount on site. Pausata et al. (2011) used a climate  
 416 model with an embedded oxygen-isotope model to simulate a Heinrich event and found that the



417 variations of stalagmite  $\delta^{18}\text{O}$  values in southern China mainly reflected  $\delta^{18}\text{O}$  changes in the  
418 source vapor from the Indian Ocean rather than local precipitation amount. Liu et al. (2015) also  
419 indicated that the stalagmite  $\delta^{18}\text{O}$  records during the Holocene from the East Asian summer  
420 monsoon region are essentially a signal of the isotopic composition of precipitation, which is  
421 largely determined by the upstream depletion mechanism over the Indian Ocean and the Indian  
422 monsoon region.

423 As a result, the upstream rainout effect associated with the convective processes over the  
424 moisture source region is likely an important factor that affects the isotopic variability in the  
425 Asian summer monsoon precipitation. However, a correlation between the  $\delta^{18}\text{O}$  and precipitation  
426 amount in the summer of 2013 (Fig. 6b) seemed to suggest that the amount effect could still play  
427 an important role, particularly during the periods when precipitation varied greatly such as the  
428 glacial-interglacial climate cycles. In addition, there is likely considerable amount of local  
429 evapotranspiration in the Asian monsoon region because of high vegetation cover under humid  
430 monsoon climate conditions. How the local evapotranspiration affects the summer precipitation  
431  $\delta^{18}\text{O}$  is still unclear and requires further study.

432 The linear slope (0.16‰/°C) between the daily surface air temperature and  $\delta^{18}\text{O}$  in  
433 non-monsoonal precipitation is consistent with the slope (0.20‰/°C) calculated by the monthly  
434 isotopic and air temperature data of Nanjing during the non-monsoon season obtained from the  
435 Global Network for Isotopes in Precipitation (GNIP) at <http://isohis.iaea.org/gnip.asp>. This  
436 confirms the temperature effect of stable isotopes in the non-monsoon season. By contrast, the  
437 correlation between surface air temperature and non-monsoonal precipitation  $\delta^{18}\text{O}$  of Nanjing is  
438 weaker than the correlation in high latitudes. This may be caused by changes in moisture source

439 of the remote moisture deriving from the inland of Eurasia versus the proximal moisture  
440 originating in the China offshore seas (Fig. 3). In addition, the effect of potential re-evaporation  
441 of precipitation on isotopic composition of precipitation during its falling due to relatively dry  
442 climate condition in the non-monsoon season could also contribute to the weak temperature  
443 effect of stable isotopes. Anyhow, the considerable precipitation amount in the non-monsoon  
444 season highlights the importance of the temperature effect for interpretation of stable isotope  
445 records in speleothems from the monsoon region. Some studies demonstrated that winter  
446 temperature in East China was dominated by the East Asian winter monsoon associated with the  
447 Mongolia High (Guo, 1994; Liu et al., 2011).

448 As a result, the isotopic composition of precipitation, which was preserved in stable oxygen  
449 isotope records from speleothems in the East Asian monsoon region, should be controlled by  
450 both the East Asian summer monsoon and the East Asian winter monsoon. Indeed, Clemens et al.  
451 (2010) suggested that the timing of light  $\delta^{18}\text{O}$  peaks in speleothems from Southeast China at the  
452 orbital time scale were controlled by both strong summer monsoons and winter temperature  
453 changes. Other studies suggest that the oxygen isotope records in Chinese speleothems indicate  
454 changes in the ratio of summer to winter precipitation (Wang et al., 2001; Yuan et al., 2004;  
455 Dykoski et al., 2005; Kelly et al., 2006; Wang et al., 2008; Zhang et al., 2008; Cheng et al., 2009).  
456 However, this inference lacks theoretical basis because influencing factors on stable isotopes of  
457 precipitation were not taken into account. Indeed, there was no correlation between the annual  
458 mean weighted-precipitation  $\delta^{18}\text{O}$  and the ratio of summer to winter precipitation based on  
459 modern observations of precipitation stable isotopes data from GNIP Nanjing station and our  
460 study (figure not shown, the year with lack observation more than two months was not included

461 for statistical analysis).

462 In summary, for improving the interpretation of the oxygen isotopic records in speleothems  
463 in the Asian monsoon region at longer time scales such as the glacial-interglacial climate cycles,  
464 the upstream rainout on stable isotopes related to changes of the Asian summer monsoon and the  
465 temperature effect associated with winter monsoon should be considered, which could be  
466 evaluated by present-day and past simulations of water stable isotopes in the general circulation  
467 models (Risi et al., 2010; Werner et al., 2011).

468

## 469 **6 Conclusions**

470 We emphatically analyzed daily stable isotopic composition of summer precipitation in  
471 Nanjing in 2012–2014, and related it to OLR and water vapor transport data to identify the  
472 influence of ITCZ location and intensity on the stable isotopic composition of precipitation. At  
473 the onset of the summer monsoon (stage 1), vapor to our study site was mainly transported from  
474 the **Bay of Bengal**, where the strong convection in the source area and its relatively long distance  
475 from our study area acted to reduce  $\delta^{18}\text{O}$  in precipitation in Nanjing. During the Meiyu period  
476 (stage 2), water vapor came mainly from the **South China Sea**, and changes in ITCZ intensity in  
477 the **South China Sea** led to the variability of  $\delta^{18}\text{O}$  in precipitation in Nanjing. The northward  
478 propagation of the ITCZ during the mid-monsoon season (stage 3) reduced the vapor transport  
479 distance, resulting in relatively enriched  $\delta^{18}\text{O}$ . During the late monsoon period (stage 4), the  
480 ITCZ retreated to the **Bay of Bengal**. The strong convection and relatively long-distance vapor  
481 transport again led to depleted  $\delta^{18}\text{O}$  values in precipitation in Nanjing. Finally, when the  
482 monsoon withdrew (stage 5), vapor from the north and west inland areas contributed to the

483 enriched  $\delta^{18}\text{O}$ .

484 Our study indicates that the changes in the ITCZ location and intensity are major factors  
485 affecting the stable isotopes in summer precipitation in Nanjing. Therefore, the stable isotopes in  
486 precipitation could signal a shift of precipitation source regions and ITCZ over the course of  
487 monsoon season. As a result, changes in moisture sources and upstream rainout effect should be  
488 taken into account when interpreting the stable isotopic composition of speleothems in the Asian  
489 monsoon region. However, the temperature effect of stable isotopes is also important for  
490 interpreting the stable isotopic composition of speleothems in the Asian monsoon region because  
491 of almost half annual precipitation occurring in the non-monsoon season.

492

#### 493 **Acknowledgments**

494 We thank the NOAA Air Resources Laboratory (ARL) for providing the HYSPLIT model  
495 used in this study. This work was supported by the Natural Science Foundation of China  
496 (41330526, 41171052 and 41321062) and the Priority Academic Program Development of  
497 Jiangsu Higher Education Institutions (PAPD).

498

#### 499 **References:**

500 Ananthakrishnan, R., Pathan, J. M., and Aralikatti, S. S.: On the northward advance of the ITCZ  
501 and the onset of the southwest monsoon rains over the southeast Bay of Bengal, Int. J.  
502 Climatol., 1,153-165, 1981.

503 Araguas-Araguas, L., Froehlich, K., and Rozanski, K.: Stable isotope composition of  
504 precipitation over southeast Asia, J. Geophys. Res., 103(D22), 28721-28742, 1998.

505 Araguás-Araguás, L., Froehlich, K., and Rozanski, K.: Stable isotope composition of  
506 precipitation over Southeast Asia, *J. Geophys. Res.*, 103, D22, 721-28742, 1998.

507 Bershaw, J., Penny, S. M., and Garziona, C. N.: Stable isotopes of modern water across the  
508 Himalaya and eastern Tibetan Plateau: implications for estimates of paleoelevation and  
509 paleoclimate, *J. Geophys. Res.*, 117: D02110, doi:10.1029/2011JD016132, 2012.

510 Breitenbach, S. F. M., Adkins, J. F., Meyer, H., Marwan, N., Kumar, K. K., and Haug, G. H.:  
511 Strong influence of water vapor source dynamics on stable isotopes in precipitation observed  
512 in Southern Meghalaya, NE India, *Earth. Planet. Sci. Lett.*, 292, 212-220, 2010.

513 Brimelow, J. C. and Reuter, G. W.: Transport of atmospheric moisture during three extreme  
514 rainfall events over the Mackenzie River basin, *J. Hydrometeorol.*, 6, 423-440, 2005.

515 Cai, Y. J., Tan, L. C., Cheng, H., An, Z. S. Edwards, R. L., Kelly, M. J., Kong, X. G., and Wang,  
516 X. F.: The variation of summer monsoon precipitation in central China since the last  
517 deglaciation, *Earth Planet. Sci. Lett.*, 291, 21-31, 2010.

518 Cheng, H., Edwards, R. L., Broecker, W. S., Denton, G. H., Kong, X. G., Wang, Y. J., Zhang, R.,  
519 and Wang, X. F.: Ice Age Terminations, *Science*, 326, 248-252, 2009.

520 Clemens, S. C., Prell, W. L., and Sun, Y.: Orbital-scale timing and mechanisms driving Late  
521 Pleistocene Indo-Asian summer monsoons: Reinterpreting cave speleothem  $\delta^{18}\text{O}$ ,  
522 *Paleoceanography*, 25, PA4207, doi:10.1029/2010PA001926, 2010.

523 Conroy, J. L., Cobb, K. M., and Noone, D.: Comparison of precipitation isotope variability  
524 across the tropical Pacific in observations and SWING2 model simulations, *J. Geophys. Res.*,  
525 118, 5867-5892, 2013.

526 Cruz, F. W., Burns, S. J., Karmann, I., Sharp, W. D., Vuille, M., Cardoso, A. O., Ferrari, J. A.,

- 527 Dias, P. L. S., and Viana, O. Jr.: Insolation-driven changes in atmospheric circulation over the  
528 past 116000 years in subtropical Brazil, *Nature*, 434, 63-66, 2005.
- 529 Cruz, F. W., Vuille, M., Burns, S. J., Wang, X. F., Cheng, H., Werner, M., Edwards, R. L.,  
530 Karmann, Ivo., Auler, A. S., and Nguyen, H.: Orbitally driven east-west antiphasing of South  
531 American precipitation, *Nature Geoscience*, 2, 210-214, 2009.
- 532 Dansgaard, W.: Stable isotopes in precipitation, *Tellus*, 16, 436-468, 1964.
- 533 Dayem, K. E., Molnar, P., Battisti, D. S., and Roe, G. H.: Lessons learned from oxygen isotopes in  
534 modern precipitation applied to interpretation of speleothem records of paleoclimate from  
535 eastern Asia, *Earth Planet. Sci. Lett.*, 295, 219-230, 2010.
- 536 Ding, Y. H., Liu, J. J., Sun, Y., Liu, Y. J., He, J. H., and Song, Y. F.: A Study of the  
537 Synoptic-Climatology of the Meiyu System in East Asia, *Chinese Journal of Atmospheric  
538 Sciences (in Chinese)*, 31, 1082-1100, 2007.
- 539 Ding, Y. H.: Summer monsoon rainfall in China, *J. Meteor. Soc. Japan*, 70, 373-396, 1992.
- 540 Ding, Y. H.: The variability of the Asian summer monsoon, *J. Meteor. Soc. Japan*, 85B, 29, 2007.
- 541 Drumond, A., Nieto, R., Gimeno, L.: On the contribution of the tropical western hemisphere  
542 warm pool source of moisture to the Northern Hemisphere precipitation through a Lagrangian  
543 approach, *J. Geophys. Res.*, 16, D00Q04, doi:10.1029/2010JD15397, 2011.
- 544 Dykoski, C. A., Edwards, R. L., Cheng, H., Yuan, D. X., Cai, Y. J., Zhang, M. L., Lin, Y. S.,  
545 Qing, J. M., An, Z. S., and Revenaugh, J.: A high-resolution, absolute-dated Holocene and  
546 deglacial Asian monsoon record from Dongge Cave, China, *Earth Planet. Sci. Lett.*, 233,  
547 71-86, 2005.
- 548 **Gadgil, S.: The Indian monsoon and its variability, *Annu. Rev. Earth Planet. Sci.*, 31, 429-467,**

549 2003.

550 Gao, J., Delmotte, V. M., Risi, C., He, Y., and Yao, T. D.: What controls precipitation  $\delta^{18}\text{O}$  in the  
551 southern Tibetan Plateau at seasonal and intra-seasonal scales? A case study at Lhasa and  
552 Nyalam, *Tellus*, 65: 1-14, 2013.

553 Gu, G. J., and Zhang, C. D.: Cloud components of the Intertropical Convergence Zone, *J.*  
554 *Geophys. Res.*, 107(D21), 4565, doi:10.1029/2002JD002089, 2002.

555 Guo, Q.: Relationship between the variations of East Asian winter monsoon and temperature  
556 anomalies in China, *Quarterly Journal of Applied Meteorology*, 5(2), 218-225, 1994 (in  
557 Chinese with English abstract).

558 He, Y., Risi, C., Gao, J., Masson-Delmotte, V., Yao, T., Lai, C., Ding, Y., Worden, J., Frankenberg,  
559 C., Chepfer, H., and Cesana, G.: Impact of atmospheric convection on south Tibet summer  
560 precipitation isotopologue composition using a combination of in situ measurements, satellite  
561 data, and atmospheric general circulation modeling, *J. Geophys. Res. Atmos.*, 120, 3852-3871,  
562 doi:10.1002/2014JD022180, 2015.

563 Hu, C. Y., Henderson, G. M., Huang, J. H., Xie, S. C., Sun, Y., and Johnson, K. R.: Quantification  
564 of Holocene Asian monsoon rainfall from spatially separated cave records, *Earth Planet. Sci.*  
565 *Lett.*, 266, 221-232, 2008.

566 Kelly, M. J., Edwards, R. L., Cheng, H., Yuan, D. X., Cai, Y. J., Zhang, M. L., Lin, Y. S., and An,  
567 Z. S.: High resolution characterization of the Asian Monsoon between 146,000 and 99,000  
568 years B.P. from Dongge Cave, China and global correlation of events surrounding Termination  
569 II, *Palaeogeogr. Palaeoclimatol. Palaeoecol.*, 236, 20-38, 2006.

570 Kurita, N., Ichiyanagi, K., Matsumoto, J., Yamanaka, M. D., and Ohata, T.: The relationship

571 between the isotopic content of precipitation and the precipitation amount in tropical regions. *J.*  
572 *Geochem. Explor.*, 102, 113-122. 2009.

573 Kurita, N.: Origin of Arctic water vapor during the ice-growing season, *Geophys. Res. Lett.*, 38,  
574 L02709, doi:10.1029/2010GL046064, 2011.

575 Kurita, N.: Water isotopic variability in response to mesoscale convective system over the  
576 tropical ocean, *J. Geophys. Res.*, 118, 10376-10390, 2013.

577 Lau, K. M. and Yang, S.: Climatology and interannual variability of the Southeast Asian summer  
578 monsoon, *Adv. Atmos. Sci.*, 14, 141-162, 1997.

579 Lau, K. M., Kim, and Yang, S.: Dynamical and boundary forcing characteristics of regional  
580 components of the Asian summer monsoon, *J. Climate.*, 13, 2461-2482, 2000.

581 Lawrence, J. R. and Gedzelman, S. D.: Low stable isotope ratios of tropical cyclone rains,  
582 *Geophys. Res. Lett.*, 23, 527-530, 1996.

583 Lawrence, J. R., Gedzelman, S. D., Dexheimer, D., Cho, H. K., Carrie, G. D., Gasparini, R.,  
584 Anderson, C. R., Bowman, K. P., and Biggerstaff, M. I.: Stable isotopic composition of water  
585 vapor in the tropics, *J. Geophys. Res.*, 109, D06115, doi:10.1029/2003JD004046, 2004.

586 Lekshmy, P. R., Midhum, M., Ramesh, R., and Jani, R. A.:  $^{18}\text{O}$  depletion in monsoon rain relates  
587 to large scale organized convection rather than the amount of rainfall, *Scientific Reports*, 4,  
588 5661, doi:10.1038/srep05661, 2014

589 Liu, J., Chen, J., Zhang, X., Li, Y., Rao, Z., and Chen, F.: Holocene East Asian summer monsoon  
590 records in northern China and their inconsistency with Chinese stalagmite  $\delta^{18}\text{O}$  records,  
591 *Earth-Science Reviews*, 148, 194-208, 2015.

592 Liu, Q., Wang, P., Xu, X., Zhi, H., and Sun, X.: A group of circulation indices of Mongolia High



593 and analysis of its relationship with simultaneous anomaly in the climate of China, *Journal of*  
594 *Tropical Meteorology*, 27(6), 889-898, 2011 (in Chinese with English abstract).

595 Moerman, J. W., Cobb, K. M., Adkins, J. F., Sodemann, H., Clark, B., and Tuen, A. A.: Diurnal  
596 to interannual rainfall variations in northern Borneo driven by regional hydrology, *Earth*.  
597 *Planet. Sci. Lett.*, 369, 108-119, 2013.

598 Oh, T. H., Kwon, W. T., and Ryoo, S. B.: Review of the researches on Changma and future  
599 observational study (KORMEX), *Adv. Atmos. Sci.*, 14, 207-222, 1997.

600 Pang, H. X., He, Y. Q., Lu, A. G., Zhao, J. D., Ning, B. Y., Yuan, L. L., and Song, B.:  
601 Synoptic-scale variation of  $\delta^{18}\text{O}$  in summer monsoon rainfall at Lijiang, China, *Chin. Sci.*  
602 *Bull.*, 51, 2897-2904, 2006.

603 Pang, H., Hou, S., Kaspari, S., and Mayewski, P. A.: Influence of regional precipitation patterns  
604 on stable isotopes in ice cores from the central Himalayas, *The Cryosphere*, 8, 289-301, 2014.

605 Partin, J. W., Cobb, K. M., Adkins, J. F., Clark, B., and Fernandez, D. P.: Millennial-scale trends  
606 in west Pacific warm pool hydrology since the Last Glacial Maximum, *Nature*, 449, 452-455,  
607 2007.

608 Paulsen, D. E., Li, H. C., and Ku, T. L.: Climate variability in central China over the last 1270  
609 years revealed by high-resolution stalagmite records, *Quatern. Sci. Rev.*, 22, 691-701, 2003.

610 Pausata, F. S., Battisti, D. S., Nisancioglu, K. H., Bitz, C. M., 2011. Chinese stalagmite  $\delta^{18}\text{O}$   
611 controlled by changes in the Indian monsoon during a simulated Heinrich event. *Nat. Geosci.*  
612 4, 474-480.

613 Peng, T. R., Wang, C. H., Huang, C. C., Fei, L. Y., Chen, C. T. A., and Hwong, J. L.: Stable  
614 isotopic characteristic of Taiwan's precipitation: A case study of western Pacific monsoon

615 region, *Earth Planet. Sci. Lett.*, 289, 357-366, 2010.

616 Perry, L. B., Konrad, C. E., Schmidlin, T. W.: Antecedent upstream air trajectories associated  
617 with northwest flow snowfall in the southern Appalachians, *Wea. Forecasting*, 22, 334-351,  
618 2007.

619 Qian, W. H. and Lee, D. K.: Seasonal march of Asian summer monsoon, *Int. J. Climatol.*, 20,  
620 1371-1381, 2000.

621 Risi, C., Bony, S., Vimeux, F., and Jouzel, J.: Water-stable isotopes in the LMDZ4 general  
622 circulation model: Model evaluation for present-day and past climates and applications to  
623 climatic interpretations of tropical isotopic records, *J. Geophys. Res.*, 115, D12118,  
624 doi:10.1029/2009JD013255.

625 Saito, N.: Quasi-stationary waves in mid-latitudes and Baiu in Japan, *J. Meteor. Soc. Japan*, 63,  
626 983-995, 1995.

627 Sano, M., Xu, C. X., and Nakatsuka, T.: A 300-year Vietnam hydroclimate and ENSO variability  
628 record reconstructed from tree ring  $\delta^{18}\text{O}$ , *J. Geophys. Res.*, 117, D12115,  
629 doi:10.1029/2012JD017749, 2012.

630 Simmonds, I., Bi, D., and Hope, P.: Atmospheric water vapor flux and its association with  
631 rainfall over China in summer, *J. Climate.*, 12, 1353-1367, 1999

632 Sodemann, H., Stohl, A.: Asymmetries in the moisture origin of Antarctic precipitation, *Geophys.*  
633 *Res. Lett.*, 36, L22803, doi:10.1029/2009GL040242, 2009.

634 Soderberg, K., Good, S. P., O'Connor, M., Wang, L., Ryan, K., and Caylor, K. K.: Using  
635 atmospheric trajectories to model the isotopic composition of rainfall in central Kenya,  
636 *Ecosphere*, 4(3): 1-18, 2013.

637 Tan, L. C., Cai, Y. J., Cheng, H., An, Z.S., and Edwards, R. L.: Summer monsoon precipitation  
638 variations in central China over the past 750 years derived from a high-resolution  
639 absolute-dated stalagmite. *Palaeogeogr. Palaeoclimatol. Palaeoecol.*, 280, 432-439, 2009.

640 Tian, L., Masson-Delmotte, V., Stievenard, M., Yao, T., and Jouzel, J.: Tibetan Plateau summer  
641 monsoon northward extent revealed by measurements of water stable isotopes, *J. Geophys.*  
642 *Res.*, 106, D22, 28081-28088, 2001.

643 Tierney, J. E., Russell, J. M., Huang, Y. S., Sinninghe Damsté, J. S., Hopmans, E. C., and Cohen,  
644 A. S.: Northern hemisphere controls on tropical southeast Africa climate during the past 60000  
645 years, *Science*, 322, 252-255, 2008.

646 Tremoy, G., Vimeux, F., Mayaki, S., Souley, I., Cattani, O., Risi, C., Favreau, G., and Oi, M.: A  
647 1-year long  $\delta^{18}\text{O}$  record of water vapor in Niamey (Niger) reveals insightful atmospheric  
648 processes at different timescales, *Geophys. Res. Lett.*, 39, L08805,  
649 doi:10.1029/2012GL051298, 2012.

650 Vimeux, F., Tremoy, G., Risi, C., and Gallaire, R.: A strong control of the South American  
651 SeeSaw on the intra-seasonal variability of the isotopic composition of precipitation in the  
652 Bolivian Andes, *Earth. Planet. Sci. Lett.*, 307, 47-58, 2011.

653 Vuille, M., Werner, M., Bradley, R. S., and Keimig, F.: Stable isotopes in precipitation in the  
654 Asian monsoon region, *J. Geophys. Res.*, 110, D23108, doi:10.1029/2005JD006022, 2005.

655 Vuille, M., Werner, M., Bradley, R. S., and Keimig, F.: Stable isotopes in precipitation in the  
656 Asian monsoon region, *J. Geophys. Res.*, 110, D23108, doi: 10.1029/2005JD006022, 2005.

657 Wang, B. and Lin, H.: Rainy season of the Asian-Pacific summer monsoon, *J. Climate*, 15,  
658 386-398, 2002.

659 Wang, B. and Xu, X. H.: Northern Hemisphere summer monsoon singularities and climatological  
660 intraseasonal oscillation, *J. Climate*, 10, 1171-1185, 1997.

661 Wang, Y. J., Cheng, H., Edwards, R. L., An, Z. S., Wu, J. Y., Chen, C. C., and Dorale, J. A.: A  
662 high-resolution absolute-dated Late Pleistocene Monsoon record from Hulu Cave, China,  
663 *Science*, 294, 2345-2348, 2001.

664 Wang, Y. J., Cheng, H., Edwards, R. L., Kong, X. G., Shao, X. H., Chen, S. T., Wu, J. Y., Jiang, X.  
665 Y., Wang, X. F., and An, Z. S.: Millennial-and orbital-scale changes in the East Asian  
666 Monsoon over the past 224,000 years, *Nature*, 451, 1090-1093, 2008.

667 Werner, M., Langebroek, P. M., Carlsen, T., Herold, M., and Lohmann, G.: Stable water isotopes  
668 in the ECHAM5 general circulation model: Toward high-resolution isotope modeling on a  
669 global scale, *J. Geophys. Res.*, 116, D15109, doi:10.1029/2011JD015681.

670 Xie, L. H., Wei, G. J., Deng, W. F., and Zhao, X. L.: Daily  $\delta^{18}\text{O}$  and  $\delta\text{D}$  of precipitations from  
671 2007 to 2009 in Guangzhou, South China: Implications for changes of moisture sources, *J.*  
672 *Hydrol.*, 400, 477-489, 2011.

673 Yang, X. X., Yao, T. D., Yang, W. L., Xu, B. Q., He, Y., and Qu, D. M.: Isotopic signal of earlier  
674 summer monsoon onset in the Bay of Bengal, *J. Climate*, 25, 2509-2515,  
675 doi:10.1175/JCLI-D-11-00180.1, 2012.

676 Yuan, D. X., Cheng, H., Edwards, R. L., Dykoski, C. A., Kelly, M. J., Zhang, M. L., Qing, J. M.,  
677 Lin, Y. S., Wang, Y. J., Wu, J. Y., Dorale, J. A., An, Z. S., and Cai, Y. J.: Timing, duration and  
678 transition of the last interglacial Asian monsoon, *Science*, 304, 575-578, 2004.

679 Zhang, P. Z., Cheng, H., Edwards, R. L., Chen, F. H., Wang, Y. J., Yang, X. L., Liu, J., Tan, M.,  
680 Wang, X. F., Liu, J. H., An, C. L., Dai, Z. B., Zhou, J., Zhang, D. Z., Jia, J. H., Jin, L. Y., and

681 Johnson, K. R.: A test of climate, sun, and culture relationships from an 1810-year Chinese  
682 cave record, *Science*, 322, 940-942, 2008.